Damages Assessment of Cement-Paste and Cobblestone Interfacial Transition Zone by Acoustic Emission

Tam NGUYEN-TAT[1,2], *Trung-Hieu* TRAN[2], *Narintsoa* RANAIVOMANANA[1], *Jean-Paul* BALAYSSAC[1]

[1] LMDC, Université de Toulouse, INSA, UPS, France
[2] Faculty of Civil Engineering, Hanoi Architectural University, Vietnam

Abstract. In cementitious materials, bonding at the contact surface between cement-paste and coarse aggregates plays an important role and determines the durability of the material. Recent studies have evaluated the impact strength on this contact surface by experiments on different surface roughness aggregates and concluded that the contact area between the two components was the weakest zone in concrete. This paper presents experiment test on cement-paste and cobblestone contact surface to determine the types of damage modes using Acoustic Emission Technique. The result is that the shear stress occupies only about 10% of the total stress experienced on the contact surface.

1. Introduction

In concrete, the bond between the cement paste and the coarse aggregate is significant because it affects to the strength of the material. Study on the affections of aggregate surface on adhesion force with cement paste and mortar in the experiments under compress, tensile and shear samples have been published recently [1]-[5]. And damages at the contact area between cement paste and coarse aggregate or Interfacial Transition Zone (ITZ) are interested the authors in those experiments. By damage analysis of ITZ, some remarkable results have been introduced.

The failure mechanism of the ITZ between cobblestone aggregate and mortar was investigated by under the combined of normal and shear stresses [2]. Prism specimens were casted in 50×50×200 mm3 molds with marble aggregate placed in the molds and the interface inclination angles were 45 degrees. It was concluded that the shear bond strength of the interface was approximated to the shear strength of the mortar.

The affection of surface roughness to the bonding strength of the ITZ between coarse aggregates and mortar and on the damage processes of concrete under uniaxial tensile and uniaxial compression were presented [3]. Five kinds of surfaces have made: fully polished, medium polished, saw-cut, sandblasted, and notched surfaces. As conclusion, when the normal stress lower than 60% of the mortar compressive strength, the tensile and shear bond strengths of the interface increased with increased surface roughness of aggregates, and also resulted in rising of concrete splitting tension strength.

The shear failure process of the ITZ of the granite - mortar specimens have been monitored by the Acoustic Emission (AE) system [4]. Cylinder specimens with 64mm diameter including three layers: mortar, granite and mortar were conducted by direct shear tests. Failure processes at the contact surface are recorded with the AE signals obtained. The parameters of these signals showed that the AE technique was appropriate for the experiments and it also indicated the damage severity of the samples.

Recently, the mechanical properties of the cement paste - aggregate specimens were experimentally studied [5]. These samples were composed of limestone aggregates and Portland cement paste which dimension of 10×10×30 mm3. The results showed that the cement-aggregate interface is the weakest zone in concrete, this is good agreement with that in [6]. The authors also concluded that if the normal force is applied to the shear samples, the shear strength value increases significantly.

In general, the above ITZ studies between cement paste and aggregate have assessed the affections of surface roughness to bonding as well as on the tensile and compressive strengths of the material at the interfaces. Therefore, studies on the types of damage modes occurring on the surface of contact between the two materials need further study. In this paper, the author presents an experiment test to determine the damage modes on cement paste exposed to cobblestone by Acoustic Emission Technique (AET). The results showed that the stresses at ITZ include both modes I and mode II, and the proportion of mode I is significantly higher than that in mode II.

2. Experimental methodology and acquirement system

2.1 Specimen setup

The specimen namely CPRI (Cement-Paste and Rock Interface) has dimension of 60×60×120 mm3 and consists of two parts; the lower part is a block of cobblestone, a common aggregate for concrete, with a 45 degree surface that created by saw cut. The above cement-paste is poured into the lower part at the incline surface and maintained in the laboratory 28 days before conduct the experiment test. In cement-paste, the type I Portland cement [7] was used with the water/cement ratio is 3.0. The mechanical properties were determined at 28 days on three 118×225 mm2 cylinders. Compressive strength (f_c') of 68.9 MPa was assessed by direct compression tests based on EN 12390-3 [8]; the Elastic modulus of 23.6 GPa was determined according to RILEM CPC8 recommendation [9].

The specimen was subjected to compression test to verify the fracture modes in the cement-paste and cobblestone interface under monotonic loading. To produce shear damage at cement-paste and cobblestone contact (shear damage under compression test), notches with 20mm depth were created surround this interface boundary. The loading was controlled by a rate 50 N/s.

2.2 Acoustic Emission acquirement setup

The Acoustic Emission (AE) is a common non-destructive testing method that used to (i) locate the micro-cracks, (ii) characterize the damage modes, and (iii) to assess the damage severity of the construction structures. Some AE parameters can be directly extracted from one signal such as the Count, the Amplitude, the Duration, the Rise-Time, the Energy, etc. These are called primary parameters [10]. By damage mode classification applying RA method, the mode I cracks result in waveforms with short Rise-Time and high Average Frequency whereas mode II cracks result in waveforms with longer Rise-Time and lower Average Frequency. The Rise-Time and the maximum Amplitude are used to calculate RA value, while the Average Frequency value is obtained from AE count and the Duration time [11].

AE activities were recorded by using eight-channel PCI-8 acquisition device of the Physical Acoustic Corporation (PAC). AE detection was carried out by R15- sensors PAC series with the specifications as indicated in Table 1. These sensors are mounted on the surface of the specimens with silicon grease as coupling agent, and they were placed close to the expected location of the future cracks path to minimize errors in the AE event localization.

Table 1. Specification of the R15-series.

Parameters	Operating specification
Operating frequency	50 – 400 kHz
Resonant frequency	150 kHz
Peak sensitivity	80 dB
Dimensions	19 mm (diameter) × 22.4 mm (height)

The PAC preamplifiers model 2/4/6 (gain selectable 20/40/60 dB + 5% dB) apply a gain of 40 dBs to eliminate the background noise. The acquisition system was calibrated before each test using a standard source Pencil Lead Break (PLB) procedure Hsu-Nielsen, and to verify that nothing has changed on sensors sensitivity before and after the test, the Auto Sensor Test was performed. In these tests, the AE events are located by applying the wave propagation velocity of 3,900 m/sec. AE detection was performed by means of six sensors that fixed on the sample as presented in (a) Testing specimen (b) Specimen at failure

Fig. 1(a). The three-dimension Cartesian coordinates of the sensors are indicated in Table 2. (a) Testing specimen (b) Specimen at failure

Fig. **1**(b) introduces the sample after the experiment; the slip damage was occurred at the contact surface between cement-paste and cobblestone and split the sample into two parts.

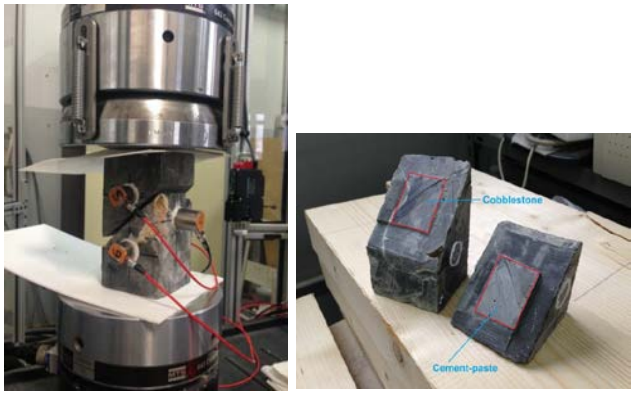

(a) Testing specimen (b) Specimen at failure

Fig. 1. Sensors arrangement on specimen (a), and specimen at failure (b).

Table 2. AE sensors arrangement.

No.	X (cm)	Y (cm)	Z (cm)
1	3	8	6
2	0	10	3
3	0	5	3
4	3	7	0
5	6	9	3
6	6	4	3

3. Result and discussion

3.1 Evolution of mechanical damage versus AE hits

In term of mechanical, the Fig. **2** indicates the evolution of loading versus axial displacement for the tested specimen. In the first segment, loading is linear developed that representation of the elastic behavior of material, then it becomes non-linear and reaches the maximum value at final of the test. The peak loading value is 14.3 kN corresponding to axial shortening of 177 m.

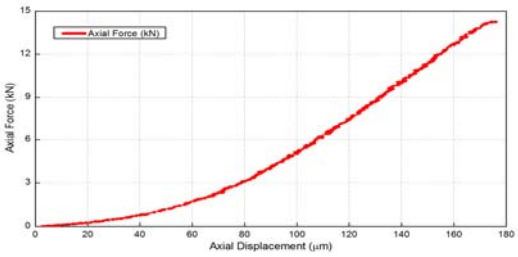

Fig. 2. Evolution of loading and displacement on CPRI specimen.

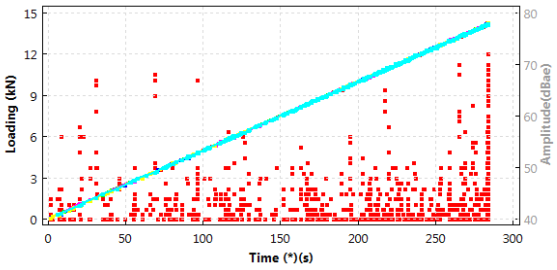

Fig. 3. Correlation of Loading and Amplitude versus time in CPRI test.

In term of AE, the Fig. **3** shows the loading curve and the number of signals obtained in the test versus time. Accordingly, AE signals were obtained immediately after the loading began but the AE number is varied during the experiment. It is noteworthy that at the peak load moment, although this is a very short time but the number of AE hits was recorded very significant and accounted for 282/984 or 28.7% of the total number of signals obtained during the experiment. The high abundant signals were collected at the peak load corresponds to the rapidly growing of the crack after the loading reaches its maximum value. In this test, specimen generated 984 signals after time t = 292 s.

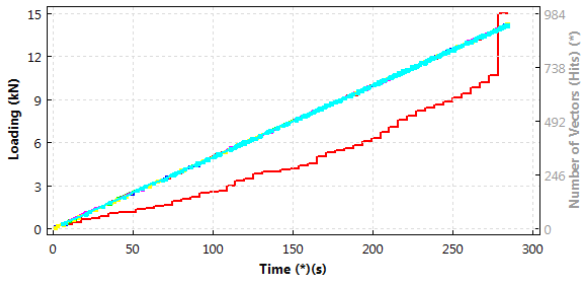

Fig. 4. Loading and cumulative AE hits vs. Time.

The amount of AE signals obtained during the test is also represented by a cumulative curve as shown in Fig. **4**. In the figure, the cumulative AE hit (the red line) is stable increased along with the development of the axial loading (the blue line). It increased dramatically at the end of the experiment when the load reached the max value and the sample was completely failure.

The number of AE signals received in the six sensors in Fig. **5** showing that the sensors CH1 to CH6 have recorded different number of signals. The CH6 obtained the most (363 signals) while CH4 obtained the least (70 signals). This difference may be due to the variation of the distance between the events and the sensors, because the sensors that farther from the events will receive lower number of signals than the closer sensors. In addition, this discrepancy may due to the influence of the notches on the sample surface to the transmission path and to reduce the amplitude of the signals leading to some sensors have not detect the signals.

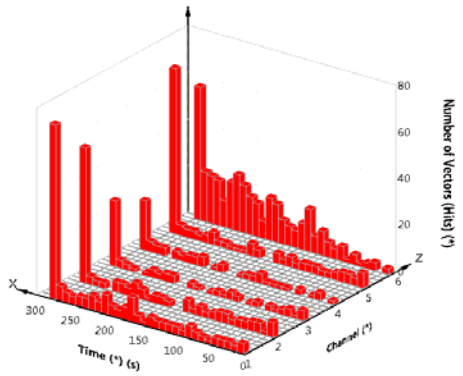

Fig. 5. Number of AE hits in Channel CH1 to CH6 vs. Time.

The cumulative ABEN (Absolute Energy) value of the signals obtained in this experiment is shown in Fig. **6**. It was found that the ABEN cumulative value from the beginning of the test to the before failure was about 150,000 aJ, and at the peak load moment (equivalent to 28.7% of the received signals), ABEN cumulative value increased to 335,991 aJ. Obviously, at the final stage before the sample is completely destroyed, the AE signals have high Amplitude as well as Energy, which may be due to large-scale fracture (or macro-crack) occurrence in the specimen.

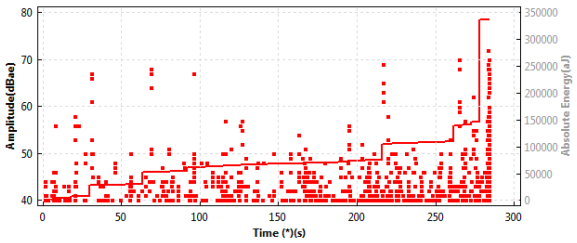

Fig. 6. Signal Amplitude and Cumulative ABEN vs. Time.

3.2 Evolution of RA and AF versus damage modes

In the experiment tests on the cementitious material applying AE technique, a damage modes classifying method using AE parameters such as Average Frequency (AF, kHz) and RA (Rise-Time per Amplitude, ms/V) is presented in RILEM TC 212-ACD [12]. In this CPRI test, the RA and AF values are calculated and displayed on the same graph as shown in Fig. **7**. Accordingly, the low RA and high AF signals are located in Zone 1, while the high RA and low AF signals are classified in Zone 2. Also in Fig. **7**, the signal in Zone 1 represents 71.7% of the total signal.

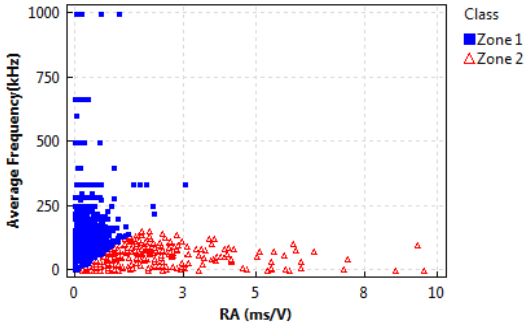

Fig. 7. Correlation between RA and AF.

To assess the other parameters of Zone 1 and Zone 2, the correlation diagrams between Rise-Time (RT) and AF, between Amplitude and AF are shown below. In Fig. **8**, the relationship between RT and AF introduces that signals are classified into two distinct areas as Zone 1 and Zone 2. This indicates that, instead of using RA and AF values, the RT and AF can be used to classify destructive modes. Signals with low RT and high AF are assigned to Zone 1 and the ones with large RT and small AF are assigned to Zone 2.

In term of Amplitude (Amp, dB), signals in Zone 1 have higher Amp value than those in Zone 2. In Fig. **9**, Zone 1 signals have Amp ranging from 40 to 80 dB while Zone 2 from 40 to 60 dB. For low Amp signals that classified into Zone 2, it is noted worthy that the distance from the sensor to the original source or event may influence to the Amp value. Because the sensors that farther from the event than others may receive low Amp signals due to amplitude attenuation versus travelling distance [13].

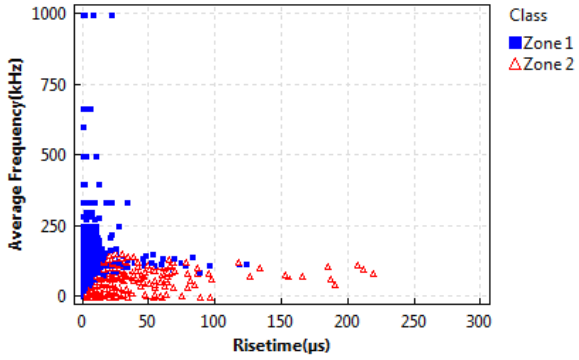

Fig. 8. Correlation between RT and AF.

The following content related to the occurrence of the signals in Zone 1 and Zone 2 versus the experimental time. The Fig. **10** shows that the signals from both groups were appeared from the beginning of the experiment, and the sudden accelerate at the moment before the final failure. In the graph, the RT value of Zone 2 is higher than that of Zone 1.

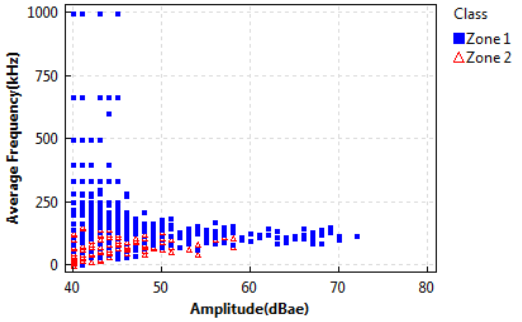

Fig. 9. Correlation between Amplitude and AF.

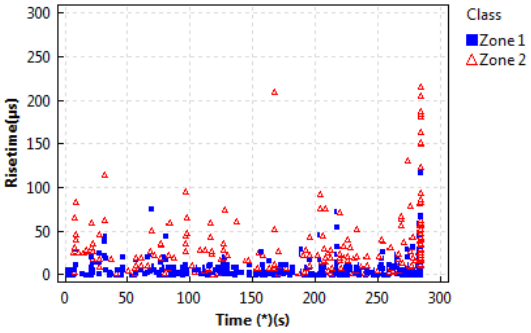

Fig. 10. Evolution of RT vs. time.

3.3 Evolution of moving average 100-hit RA and AF versus damage modes

In the light of RILEM TC 212-ACD [12], the shear-induced damage under compression test on CPRI were performed to verify the stress proportion at ITZ between cement-paste and cobblestone. The RA method is applied to classify the damage modes in the samples. And as recommended by [12], the RA and AF values should be calculated from moving average of more than 50 continuous hits. In this test, authors obtained these two features by determining the moving average of 100 continuous signals.

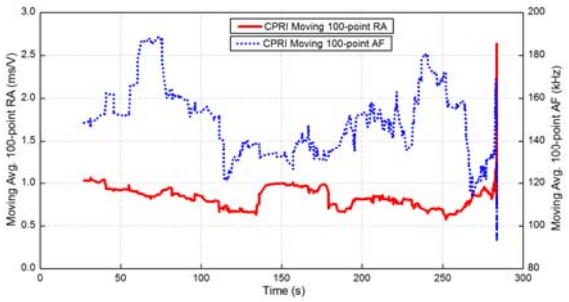

Fig. 11. Evolution of moving average continuous 100-point RA and AF.

The Fig. **11** shows the variation of RA and AF that determined from the moving average 100 continuous points in the CPRI test. As can be seen, the first phase, from the beginning to the moment before the final failure, the RA values are fluctuated in a range from 0.5 to 1.2 ms/V. At the final phase, the RA rises dramatically to 2.7 ms/V and the sample is completely failure. In term of

AF feature, in the first stage, AF fluctuated in the range of 120 to 190 kHz. At failure period, AF dropped rapidly to 90 kHz and the CPRI sample was completely failure. Thus, before the final failure, the RA value increased and higher than 1.2 ms/V while AF dropped and lower than 120 kHz corresponding to the failure moment in Fig. **11**. The damage mode in this final period corresponding to shear mode that good agreement with [14].

3.4 Crack classification using RA method: results and analysis

The testing process in the CPRI is divided into two phases in Fig. **12**; in Phase 1, RA fluctuates in the range of 0.5 to 1.2 ms/V and AF is in the range of 120 to 190 kHz. In the next Phase, RA increases from 1.2 ms/V to 2.7 ms/V, while AF decreases from 120 kHz to 90 kHz. At this Phase, the cracks grow rapidly and the sample completely failure. Thus, in the shear-induced test on CPRI specimen, the damages in the first Phase can be classified as mode I, while mode II is classified to final Phase. The breakdown of two damage phases is shown in Fig. **12**, where the diagonal line has a ratio K = 3/300 = 1/100. The intersection points at the two phases are the transition between the two damage states, from mode I to mode II or from mode II to mode I.

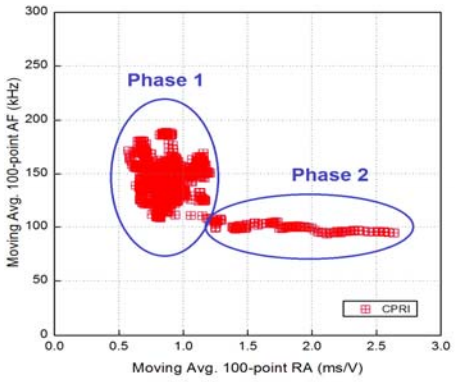

Fig. 12. Damage classification in tensile specimens.

If we accept the damage classification by the transition from mode I to mode II at the ratio of 1/100 as indicated by the diagonal line on the Fig. **12**, the following proportion of damage modes in tested specimen can be obtained. Phase 1, from beginning to before final state, the damage state is pure mode I. At failure moment (Phase 2), shear mode appears and quickly accelerate then dominant of 100% of the stresses. Comparing to the total received signals; the shear mode is occupied 10% of the total damage modes.

4. Conclusion

Aim to produce shear failure in cement-paste and cobblestone interfacial specimen under compression loading; the pre-notches are placed surround the contact surface to promote shear fracture. However, by the classification method based on RA and AF which determined from the moving average 100 moving signals, the results show that the cracks in the tested specimen are caused by the dominant tensile stress. The shear stress appeared at the final moment, in which the sample was completely failure, and the rate of mode II was about 10% to the total of the signals that obtained during the test.

References

1. W. A. Tasong, C. J. Lynsdale, J. C. Cripps, Aggregate-cement paste interface Part I. Influence of aggregate geochemistry, C.C.R. 29 (1999) 1019–1025.
2. X. Gu, L. Hong, Z. Wang, F. Lin, Experimental study and application of mechanical properties for the interface between cobblestone aggregate and mortar in concrete, C.B.M. 46 (2013) 156–166.
3. L. Hong, X. Gu, F. Lin, Influence of aggregate surface roughness on mechanical properties of interface and concrete, C.B.M. 65 (2014) 338–349
4. Y. Wang, S. J. Chen, H. T. Zhao, Y. Z. Chen, Acoustic emission characteristics of interface between aggregate and mortar under shear loading, Russ. J. Nondestruct. Test. 51 (2015) 497–508.
5. M. Jebli, F. Jamin, E. Malachanne, E. Garcia-Diaz, M.S. E. Youssoufi, Experimental characterization of mechanical properties of the cement-aggregate interface in concrete, C.B.M. 161 (2018) 16–25.
6. J. J. Zheng, C. Q. Li, X. Z. Zhou, Thickness of interfacial transition zone and cement content profiles around aggregates, Mag. Concr. Res. 57 (2005) 397–406.
7. ASTM C150/C150M − 15, Standard Specification for Portland Cement (2015)
8. European Standard, EN 12390-3, Testing hardened concrete - Part 3: Compressive strength of test specimens (2012)
9. RILEM TC CPC 8, Modulus of elasticity of concrete in compression, (1975)
10. C. Grosse, M. Ohtsu, eds., Acoustic Emission Testing, Springer Berlin Heidelberg, (2008)
11. RILEM Technical Committee, Test method for classification of active cracks in concrete structures by AE, Mater. Struct. 43 (2010) 1187–1189.
12. K. Ohno, M. Ohtsu, Crack classification in concrete based on acoustic emission, C.B.M. 24 (2010) 2339–2346.
13. D.G. Aggelis, A.C. Mpalaskas, D. Ntalakas, T.E. Matikas, Effect of wave distortion on acoustic emission characterization of cementitious materials, C.B.M. 35 (2012) 183–190.
14. A. Behnia, H. K. Chai, T. Shiotani, Advanced structural health monitoring of concrete structures with the aid of acoustic emission, C.B.M. 65